

Solitary myofibroma of the lumbar vertebra in young adult

A case report with 4-year follow-up of postoperative CT or MRI

Sang Min Lee, MD, PhD^{a,*}, Doo Hoe Ha, MD^a, Haeyoun Kang, MD, PhD^b, Dong Eun Shin, MD, PhD^c

Abstract

Background: Solitary myofibroma of the spine is extremely rare, particularly among adults. To the best of our knowledge, only 3 cases affecting lumbar vertebrae have been reported in the English language literature. Of them, only 1 case was an adult case of solitary myofibroma affecting the L1 vertebra.

Methods: We report a case of solitary myofibroma affecting the L5 vertebra in an 18-year-old man and the postoperative imaging of solitary myofibroma for the first time. Conventional radiographs demonstrated an expansile osteolytic lesion with thinned cortex and marginal sclerosis. Computed tomography (CT) showed a purely osteolytic expansile lesion with partial disappearance of thinned cortex. MRI of the lesion revealed an isointense signal on T1-weighted images, an inhomogeneous slightly hyperintense signal on T2-weighted images, and homogeneous avid enhancement with gadolinium.

Results: Surgical excision was performed and the lesion was diagnosed as solitary myofibroma on pathological examination. One-year follow-up postoperative CT demonstrated decreased size of the osteolytic lesion with sclerotic change. Four-year follow-up postoperative MRI revealed complete resolution of the lesion replaced by normal fatty marrow.

Conclusion: If a benign-looking expansile osteolytic lesion reveals a homogeneously isointense signal on T1-weighted image, inhomogeneous slightly hyperintense signal on T2-weighted image, and homogeneous avid enhancement with gadolinium, solitary myofibroma should be considered in the differential diagnosis of spine bone tumors. It can be resolved completely.

Abbreviations: CT = computed tomography, MRI = magnetic resonance imaging.

Keywords: bone, computed tomography, magnetic resonance imaging, myofibroma, solitary, vertebra

1. Introduction

Myofibroma is one of the most common fibrous tumors occurring in infancy and childhood. However, it is a relatively rare neoplasm among all tumors.^[1-4] It arises either as solitary or multicentric lesions. Multicentric lesions frequently occur in infantile myofibromatosis, whereas solitary lesions tend to occur in adults usually involving superficial soft tissues.^[5-7] Solitary lesions of bones are very rare. Particularly, spine myofibroma in an adult is exceptionally rare. It occurs most commonly in boys.

Craniofacial bones are involved most frequently, followed by upper extremities and trunk. They are clinically benign. However, they can be infiltrative either radiologically or histologically.^[7] To the best of our knowledge, only 3 cases affecting lumbar vertebrae have been reported in the English language literature. Of them, 2 cases were neonate and infant cases of multicentric infantile myofibromatosis.^[8,9] Only 1 case was an adult case of solitary myofibroma affecting the L1 vertebra.^[10] In this report, we describe an extremely rare case of solitary myofibroma affecting the L5 vertebra of an 18-year-old man. Follow-up postoperative computed tomography (CT) or magnetic resonance images (MRI) are also shown.

Editor: Satyabrata Pany.

Institutional review board approval in our hospital was granted and informed consent was waived for this retrospective case report.

The authors report no conflicts of interest.

^a Department of Radiology, ^b Department of Pathology, ^c Department of Orthopedics, CHA Bundang Medical Center, CHA University, College of Medicine, Gyeonggi-do, Republic of Korea.

* Correspondence: Sang Min Lee, Department of Radiology, CHA Bundang Medical Center, CHA University, College of Medicine, 59, Yatap-ro, Bundang-gu, Seongnam-si, Gyeonggi-do 13496, Republic of Korea (e-mail: smlee@cha.ac.kr).

Copyright © 2017 the Author(s). Published by Wolters Kluwer Health, Inc. This is an open access article distributed under the terms of the Creative Commons Attribution-Non Commercial-No Derivatives License 4.0 (CCBY-NC-ND), where it is permissible to download and share the work provided it is properly cited. The work cannot be changed in any way or used commercially without permission from the journal.

Medicine (2017) 96:39(e8069)

Received: 11 February 2017 / Received in final form: 9 August 2017 / Accepted: 22 August 2017

<http://dx.doi.org/10.1097/MD.0000000000008069>

2. Case report

An 18-year-old man was admitted for spontaneously increasing lower back pain for 2 months. The patient had no history of trauma. On physical examination, there was no tenderness or neurological compromise. Straight leg raising test was negative. Deep tendon reflex showed nonspecific finding for both legs. No pathologic reflexes were found.

Conventional radiographs of the lumbar spine demonstrated an expansile osteolytic lesion with thinned cortex and marginal sclerosis in the right pedicle and transverse process of L5 extending to the right posterolateral portion of the vertebral body (Fig. 1A and B). CT revealed a purely osteolytic expansile bony destructive lesion in the right pedicle and transverse process of L5 extending to the right posterolateral portion of the vertebral body. The cortical bone was abnormally thinned and partially disappeared at the anterior, superior, and inferior margins of the

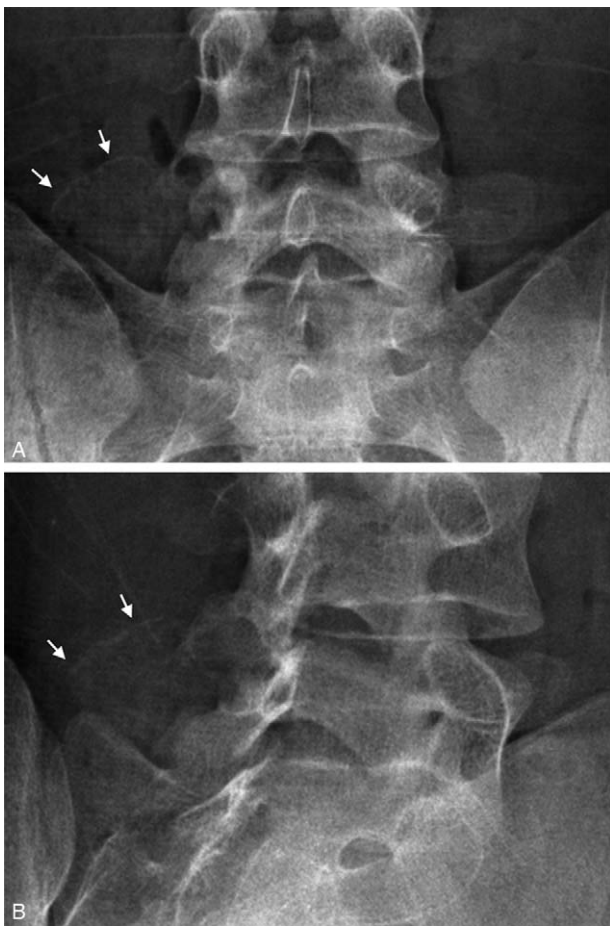


Figure 1. Conventional radiograph of the lumbar vertebra. The frontal (A) and oblique (B) views show an expansile osteolytic lesion with thinned cortex and marginal sclerosis in the right pedicle and transverse process of L5 extending to the right posterolateral portion of the vertebral body (arrows).

lesion. The lesion had a sclerotic rim in the pedicle and the right posterolateral portion of the body (Fig. 2A and B). A sharply margined osteolytic line from the lesion was extended to the articular surface of the right superior articular process of L5, suggestive of pathologic fracture involving the facet joint (Fig. 2B). Extension of the mass into adjacent vertebrae (L4, sacrum) was not observed. Enhanced CT was unavailable. MRI demonstrated an approximately $3.7 \times 3.1 \times 2.3$ cm sized mass with infiltration to the posterosuperior aspect of the right L5-S1 neural foramen through the inferior margin of the mass. Right L5 nerve root was displaced slightly downwards due to compression by the mass (Fig. 3A). The mass showed a homogeneously isointense signal with adjacent muscle on T1-weighted images (repetition time [TR]=517 ms, echo time [TE]=14 ms) (Fig. 3B) and an inhomogeneous slightly hyperintense signal on T2-weighted images (TR=4317 ms, TE=109 ms) (Fig. 3C). The mass reveals homogeneous avid enhancement on fat-suppressed T1-weighted images with gadolinium (TR=500 ms, TE=7 ms) without evidence of internal necrosis or hemorrhagic foci (Fig. 3D–F). Tc^{99m} -MDP bone scan did not demonstrate any abnormal radiotracer uptake. In the differential diagnosis of the mass, we included solid variant of aneurysmal bone cyst, osteoblastoma, and solitary myofibroma. In addition, fibrous dysplasia, histiocytosis X, desmoplastic fibroma, metastasis, and

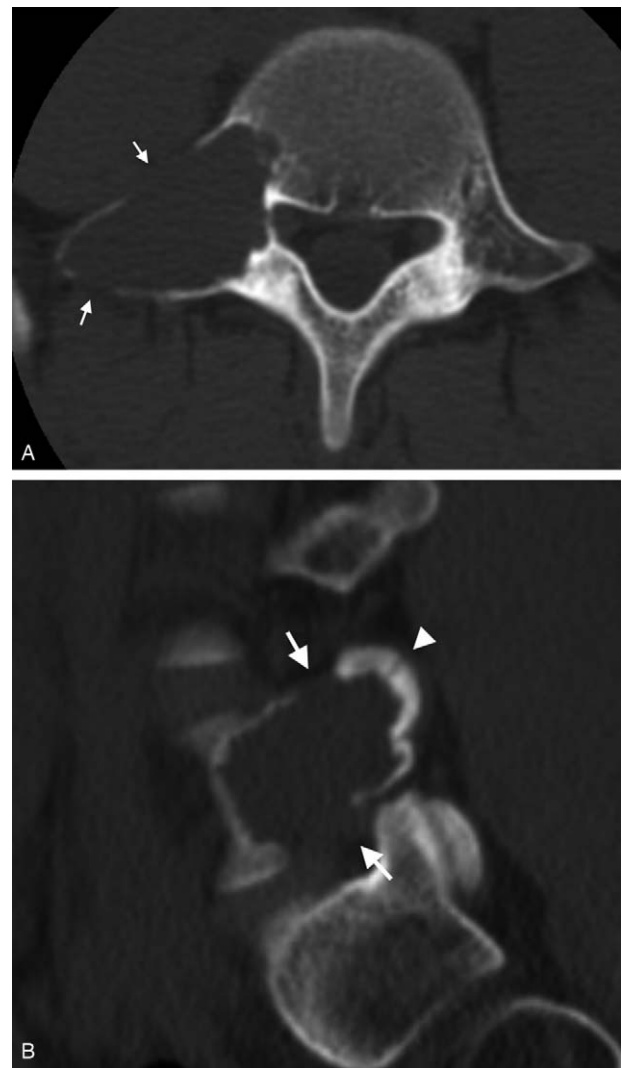


Figure 2. Computed tomography of the L5 vertebra. On axial (A) and sagittal (B) views, a purely osteolytic expansile bony destructive lesion is seen in the right pedicle and transverse process of L5 extending to the right posterolateral portion of the vertebral body. The cortical bone is abnormally thinned and partially disappeared (arrows). The lesion has a sclerotic rim in the pedicle and the right posterolateral portion of the body. A sharply margined osteolytic line from the lesion suggestive of pathologic fracture is extending to the articular surface of the right superior articular process of L5 (arrowhead).

myeloma could be contemplated in differential diagnosis of the mass.

Because the mass was an easily accessible lesion, needle biopsy was performed for accurate diagnosis and staging before surgery. Pathologically, bland spindle-shaped cells with tapering nuclei in collagenous stroma were found. More cellular areas with bundles and whorls of spindle cells showed pale eosinophilic cytoplasm associated with thin-walled branching hemangiopericytoma-like vessels. There were multifocal areas associated with pseudo-chondroid stromal hyalinization. The mass was diagnosed as a myofibroma. Because the mass had well-defined borders with cortical thinning based on radiographic characteristics of the tumor, it was stage 2 (benign active lesion) of Enneking surgical staging system. Afterward we performed marginal excision of the mass and posterior instrumentation of L4 to S1 with left-sided posterolateral fusion of L4–5 was followed because of increasing

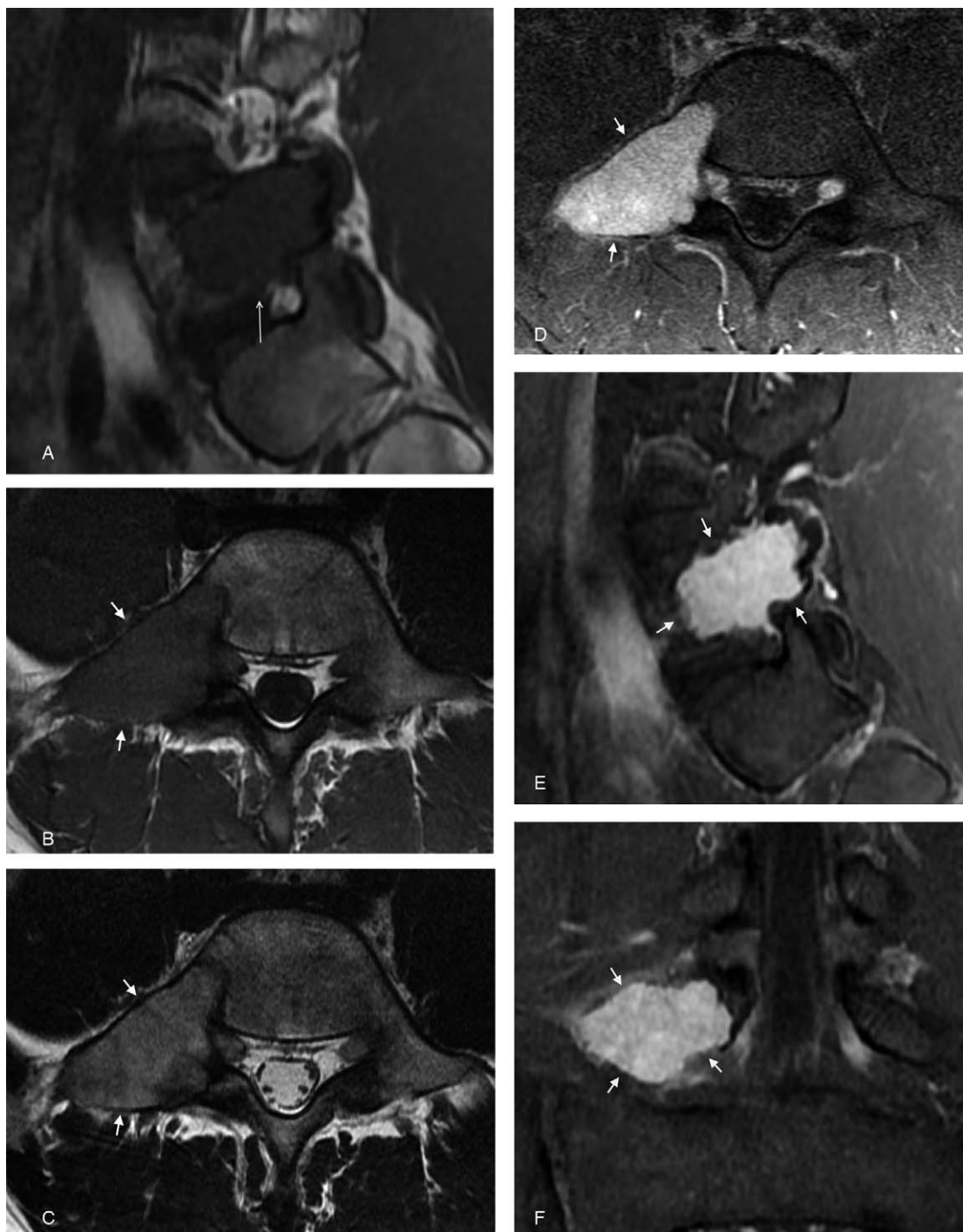


Figure 3. Magnetic resonance images of the L5 vertebra. The mass infiltrates to the posterolateral aspect of the right L5-S1 neural foramen through the inferior margin of the mass, resulting in slightly downwards displacement of right L5 nerve root (long arrow) on T1-weighted sagittal image (A). The mass (arrows) reveals homogeneously isointense signal with adjacent muscle on T1-weighted axial images (TR=517 ms, TE=14 ms) (B) and inhomogeneous slightly hyperintense signal on T2-weighted axial images (TR=4317 ms, TE=109 ms) (C). The mass (arrows) is well enhanced on fat-suppressed T1-weighted axial (D), sagittal (E), and coronal (F) images with gadolinium (TR=500ms, TE=7 ms).

lower back pain in the patient, right facet joint involvement of L4-5 by pathologic fracture and infiltration to right L5-S1 neural foramen. Adjuvant therapy such as electrocautery, burring, and phenol application was not used.

Grossly, the tumor was pinkish-white colored and solid. Microscopically, the tumor showed biphasic pattern. Cytolog-

ically, bland spindle-shaped cells with tapering nuclei in collagenous stroma were found. More cellular areas with bundles and whorls of spindle cells showed pale eosinophilic cytoplasm associated with thin-walled branching hemangiopericytoma-like vessels. There were multifocal areas associated with pseudocondroid stromal hyalinization characteristic of

myofibroma (Fig. 4A–C). Immunohistochemical staining showed positive reactions to smooth muscle actin (Fig. 4D) but negative reaction to CD34, S100 protein, and epithelial membrane antigen (EMA).

On the basis of radiological and pathological findings, we concluded that it was a solitary myofibroma originating in the right pedicle, the transverse process, and the right posterolateral body of L5.

The patient has been doing well. Follow-up CT of the lumbar spine was taken at 1 year after the operation. Follow-up CT demonstrated that the size of the osteolytic lesion was decreased with sclerotic change at the anteromedial margin of the lesion because of bony remodeling (Fig. 5A and B). There was no evidence of tumor recurrence. Hardware removal was performed after the follow-up CT at 1 year postoperatively. Several conventional radiographs of the lumbar spine were taken for a period of 3 years from the initial operation. These conventional radiographs at 3 years postoperatively showed much decreased size with obvious sclerotic change of the lesion without tumor recurrence (Fig. 5C). Follow-up MRI at 4 years postoperatively revealed complete resolution of the lesion replaced by normal fatty marrow (Fig. 5D–F).

3. Discussion

Myofibroma or myofibromatosis is known as congenital generalized fibromatosis^[11] or infantile myofibromatosis.^[12] It is the most common fibrous tumor of infancy, typically affecting neonates and children younger than 2 year of age, although it can affect older children less frequently and adults occasionally.^[13] Myofibromatosis usually involves the superficial layer of the dermis or subcutis. Deeper-seated lesions such as muscle and aponeuroses, or intraosseous lesions may also occur.^[12] Solitary

involvement of bone is very rare. It usually involves craniofacial bones. Konishi et al^[10] searched PubMed and found 44 reported cases showing solitary involvement of bone. Only 8 of these cases affected extracraniofacial bones such as femur, tibia, ulna, clavicle, sacrum, and axis.^[10,14–21] To the best of our knowledge, only 3 cases affecting lumbar vertebrae have been reported in the English language literature. Of them, 2 cases were neonate and infant cases of multicentric infantile myofibromatosis.^[8,9] Only 1 case was an adult case of solitary myofibroma affecting the L1 vertebra.^[10] No young adult case of solitary myofibroma affecting the L5 vertebra has been reported.

Radiographs and CT of solitary myofibroma of bone including the L1 vertebra usually demonstrate a well-margined purely osteolytic mass with a sclerotic rim.^[10,15,22] Expansile mass may also be accompanied by pathological fracture.^[10,14,15,18,19] MRI usually shows a hypo- to isointense signal with adjacent muscle on T1-weighted images and a homogeneous or inhomogeneous hyperintense signal on T2-weighted images with marked enhancement on postcontrast T1-weighted images.^[10,22,23] Sometimes, the mass has nonenhanced central portion, called a “target sign”, which corresponds to the presence of central necrosis on pathological examination.^[10,23]

As observed in previously reported cases, our case showed a well-demarcated, expansile, and osteolytic mass affecting the L5 vertebra with a sclerotic rim on radiographs and CT. Cortical thinning with partial loss due to cortical expansion was demonstrated with pathologic fracture. On MRI, the mass showed a homogeneously isointense signal on T1-weighted images and an inhomogeneous slightly hyperintense signal on T2-weighted images. The mass revealed homogeneous avid enhancement with gadolinium. A “target sign” presenting central necrosis was not found. These findings were compatible with those of myofibroma. However, these findings were nonspecific.

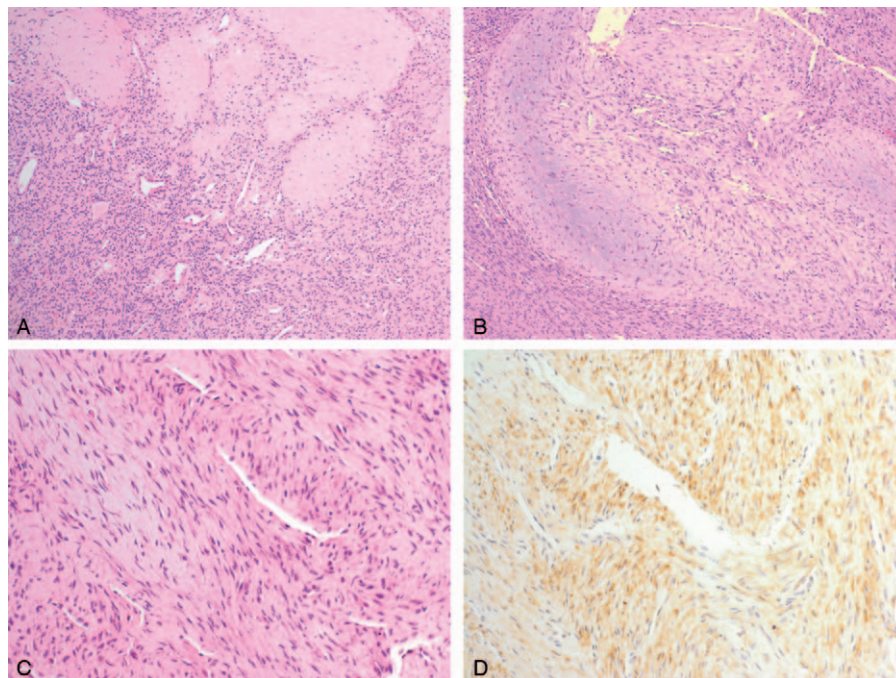


Figure 4. Histological features of solitary myofibroma of the L5 vertebra. A, Microscopically, biphasic pattern composed of spindle cells in collagenous stroma and more cellular area associated with hemangiopericytoma-like vessels are present (H&E staining; magnification $\times 40$). B, Characteristic pseudochondroid area is present (H&E staining; magnification $\times 100$). C, High power view of the tumor cells (H&E staining; magnification $\times 200$). D, Immunohistochemical staining for smooth muscle actin showing positive reaction of tumor (magnification $\times 200$).

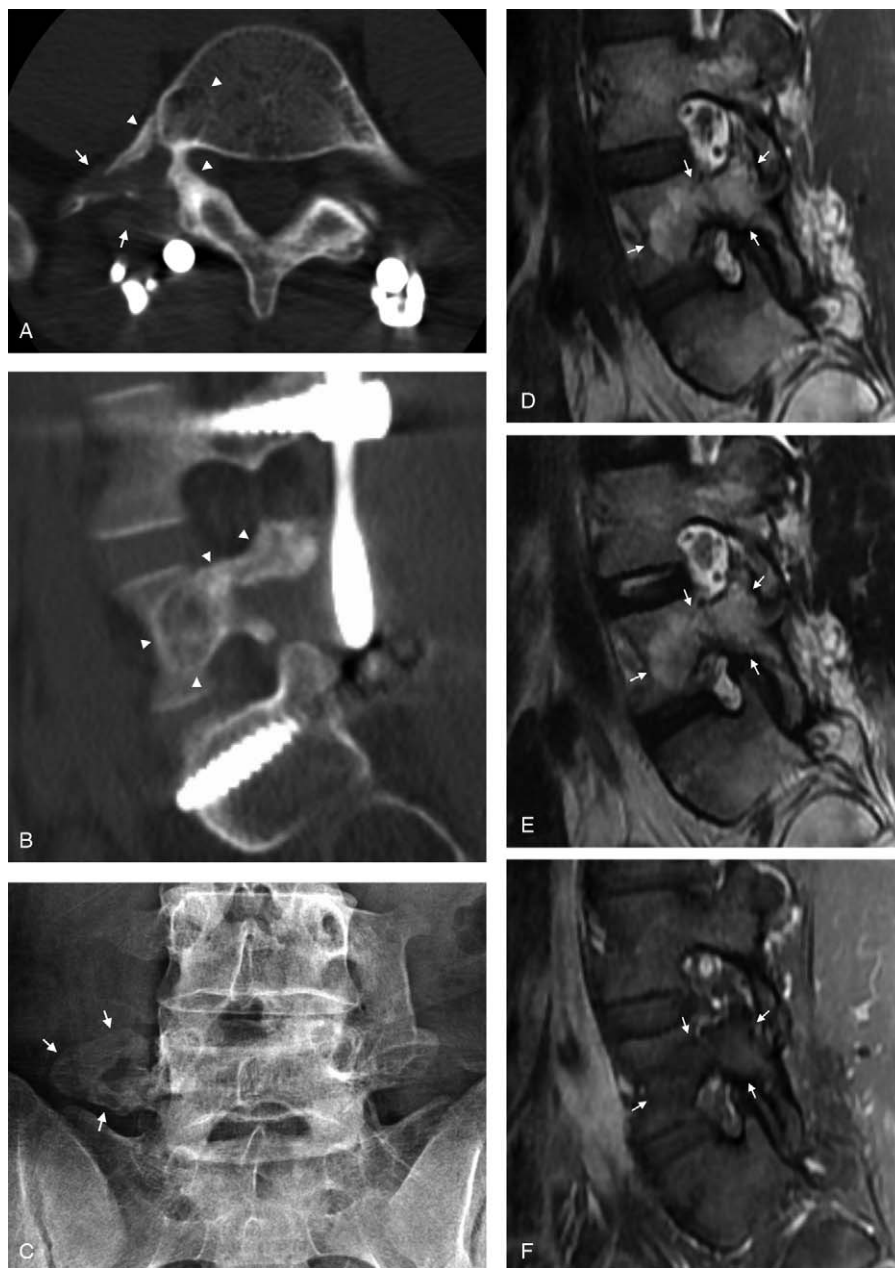


Figure 5. Postoperative images of solitary myofibroma affecting the L5 vertebra. Follow-up computed tomography (CT) of postoperative 1 year demonstrates decreased size of the osteolytic lesion (arrows) with sclerotic change at the anteromedial margin of the lesion (arrowheads) on axial (A) and sagittal (B) images. On 3-year follow-up of conventional radiograph (C), the osteolytic lesion shows much decreased size with obvious sclerotic change (arrows). Follow-up MRI of postoperative 4 years reveals complete resolution of the lesion replaced by normal fatty marrow (arrows) on T1-weighted (D) and T2-weighted (E) sagittal images as well as fat-suppressed T1-weighted sagittal image with gadolinium (F).

Therefore, solid variant of aneurysmal bone cyst and osteoblastoma appeared as well-demarcated, expansile, osteolytic lesions with a sclerotic rim were included in differential diagnoses of our case. Solid variant of aneurysmal bone cyst is seen homogeneously hypointense signal on T1-weighted images and inhomogeneously hypointense signal with scattered hyperintense signal areas on T2-weighted images with possible fluid-fluid levels, which is highly suggestive of the diagnosis of aneurysmal bone cyst.^[24] On postcontrast T1-weighted images, solid variant of aneurysmal bone cyst shows more homogeneous enhancement throughout the lesion than conventional aneurysmal bone cyst.^[24] Osteoblastoma has expansile osteolytic lesion at more

than 1.5 cm in size with little evidence of nidus calcification. It may have multiple foci of matrix mineralization or extensive sclerosis on CT sometimes. MRI of osteoblastoma demonstrates hypointense signal on T1-weighted images, mixed signal intensity on T2-weighted images due to variable matrix mineralization, and well enhancement on T1-weighted images with gadolinium.^[25] In addition, infection, fibrous dysplasia, histiocytosis X, desmoplastic fibroma, metastasis, and myeloma could be included in differential diagnosis of myofibroma.^[10]

Histologically, the differential diagnosis for the present case included solitary fibrous tumor, fibromatosis, nodular fasciitis, and neurofibroma. The features supporting the diagnosis of

myofibroma include well-defined contour, nodular biphasic pattern, characteristic pseudochondroid stromal hyalinization, and smooth muscle actin immunoreactivity.^[26]

The prognosis is generally good if the tumor does not have visceral involvement with cardiopulmonary failure, diffuse infiltration, or obstruction of the gastrointestinal tract.^[12] Complete spontaneous regression is frequently observed.^[12,27,28] Surgical excision of solitary bone lesions is usually curative. Spontaneous regression may occur in solitary bone lesions as well as soft tissue lesions.^[26] Because spontaneous regression can be expected, the first choice of management is close observation.^[8] However, in our case, we performed marginal excision of the mass and posterior instrumentation of L4 to S1 with left-sided posterolateral fusion of L4-5 because it had right facet joint involvement of L4-5 by pathologic fracture, resulting in lower back pain in patient, and infiltration to right L5-S1 neural foramen. On follow-up CT of postoperative 1 year and serial follow-up radiographs of postoperative 3 years, the osteolytic lesion showed gradually decreased size and sclerotic change which might have occurred due to bony remodeling without tumor recurrence, indicating benign lesion. Follow-up MRI of postoperative 4 years revealed complete resolution of the lesion replaced by normal fatty marrow.

In conclusion, although myofibroma usually involves the dermis or subcutis in neonates and children younger than 2 year of age, it may manifest as a benign-looking expansile osteolytic lesion in the spine with inhomogeneous slightly hyperintense signal on T2-weighted image and homogeneous avid enhancement, as in this case. Thus, it should be included in the differential diagnoses of spine bone tumors. It can be resolved completely.

References

- [1] Beck JC, Devaney KO, Weatherly RA, et al. Pediatric myofibromatosis of the head and neck. *Arch Otolaryngol Head Neck Surg* 1999;125:39–44.
- [2] Gopal M, Chahal G, Al-Rifai Z, et al. Infantile myofibromatosis. *Pediatr Surg Int* 2008;24:287–91.
- [3] Loundon N, Dedieuleveult T, Ayache D, et al. Head and neck infantile myofibromatosis—a report of three cases. *Int J Pediatr Otorhinolaryngol* 1999;51:181–6.
- [4] Josephson GD, Patel S, Duckworth L, et al. Infantile myofibroma of the nasal cavity; a case report and review of the literature. *Int J Pediatr Otorhinolaryngol* 2010;74:1452–4.
- [5] Beham A, Badve S, Suster S, et al. Solitary myofibroma in adults: clinicopathological analysis of a series. *Histopathology* 1993;22:335–41.
- [6] Swierkowski P, Seex K. Soft tissue solitary adult myofibroma in an intervertebral foramen. *ANZ J Surg* 2004;74:1028–30.
- [7] Foss RD, Ellis GL. Myofibromas and myofibromatosis of the oral region: a clinicopathologic analysis of 79 cases. *Oral Surg Oral Med Oral Pathol Oral Radiol Endod* 2000;89:57–65.
- [8] Miwa T, Oi S, Nonaka Y, et al. Rapid spontaneous regression of multicentric infantile myofibromatosis in the posterior fossa and lumbar vertebra. *Childs Nerv Syst* 2011;27:491–6.
- [9] Dautenhahn L, Blaser SI, Weitzman S, et al. Infantile myofibromatosis: a cause of vertebra plana. *AJNR Am J Neuroradiol* 1995;16(4 suppl):828–30.
- [10] Konishi E, Mazaki T, Urata Y, et al. Solitary myofibroma of the lumbar vertebra: adult case. *Skeletal Radiol* 2007;36:586–90.
- [11] Stout AP. Juvenile fibromatoses. *Cancer* 1954;7:953–78.
- [12] Chung EB, Enzinger FM. Infantile myofibromatosis. *Cancer* 1981;48:1807–18.
- [13] Wiswell TE, Davis J, Cunningham BE, et al. Infantile myofibromatosis: the most common fibrous tumor of infancy. *J Pediatr Surg* 1988;23:315–8.
- [14] Yamamoto T, Mizuno K, Hanioka K. Solitary infantile myofibromatosis in the femur. *Pathol Int* 2000;50:255–7.
- [15] Inwards CY, Unni KK, Beabout JW, et al. Solitary congenital fibromatosis (infantile myofibromatosis) of bone. *Am J Surg Pathol* 1991;15:935–41.
- [16] Bolano LE, Yngve DA, Altshuler G. Solitary fibromatosis of bone. A rare variant of congenital generalized fibromatosis. *Clin Orthop Relat Res* 1991;238–41.
- [17] Damotte D, Peuchmaur M, Padovani JP, et al. Solitary infantile myofibromatosis of bone. *Ann Pathol* 1996;16:108–11.
- [18] Kindblom LG, Angervall L. Congenital solitary fibromatosis of the skeleton: case report of a variant of congenital generalized fibromatosis. *Cancer* 1978;41:636–40.
- [19] Imaizumi S, Ogose A, Hotta T, et al. Solitary infantile myofibromatosis involving the clavicle. *Skeletal Radiol* 1999;28:473–6.
- [20] Beyer WF, Kraus J, Gluckert K, et al. Solitary infantile myofibromatosis of the sacrum. *Z Orthop Ihre Grenzgeb* 1990;128:473–6.
- [21] Asirvatham R, Moreau PG, Antonius JJ. Solitary infantile myofibromatosis of axis. A case report. *Spine (Phila Pa 1976)* 1994;19:80–2.
- [22] Tsuji M, Inagaki T, Kasai H, et al. Solitary myofibromatosis of the skull: a case report and review of literature. *Childs Nerv Syst* 2004;20:366–9.
- [23] Koujok K, Ruiz RE, Hernandez RJ. Myofibromatosis: imaging characteristics. *Pediatr Radiol* 2005;35:374–80.
- [24] Al-Shamy G, Relyea K, Adesina A, et al. Solid variant of aneurysmal bone cyst of the thoracic spine: a case report. *J Med Case Rep* 2011;5:261.
- [25] Patnaik S, Jyotsnarani Y, Uppin SG, et al. Imaging features of primary tumors of the spine: a pictorial essay. *Indian J Radiol Imaging* 2016;26:279–89.
- [26] Mentzel T, Bridge JA, Fletcher CDM, Bridge JA, Hogendoorn PCW, Mertens F. Myopericytoma, including myofibroma. *WHO Classification of Tumours of Soft Tissue and Bone 4th ed* WHO Press, IARC, Lyon:2013;118–20.
- [27] Stautz CC. CT of infantile myofibromatosis of the orbit with intracranial involvement: a case report. *AJNR Am J Neuroradiol* 1991;12:184–5.
- [28] Yoo JH, Naeini RM, Hunter JV. Infantile myofibromatosis involving the choroid plexus. *Pediatr Radiol* 2008;38:107–10.